SHEAR BEHAVIOR OF MULTI-STORY RC STRUCTURAL WALLS WITH ECCENTRIC OPENINGS

Makoto Warashina[1], Susumu Kono[2], Masanobu Sakashita[3], Hitoshi Tanaka[4]

[1] *Ex-Graduate Student, Dept. of Architecture and Architectural Engineering, Kyoto University, Kyoto, Japan*
[2] *Associate Professor, Dept. of Architecture and Architectural Engineering, Kyoto University, Kyoto, Japan*
[3] *Assistant Professor, Dept. of Architecture and Architectural Engineering, Kyoto University, Kyoto, Japan*
[4] *Professor, Disaster Prevention Research Institute, Kyoto University, Uji, Japan*
Email: kono@archi.kyoto-u.ac.jp, sakashita@archi.kyoto-u.ac.jp, tanaka@sds.dpri.kyoto-u.ac.jp

ABSTRACT :

Static loading test was conducted on four 40%-scale specimens in order to evaluate the shear transfer mechanisms of structural walls with eccentric openings. Specimen configuration was determined from a typical six-story building in Japan. The experimental variables were the size and location of openings. From experimental results, shear strength of specimens were estimated using the existing codes and reduction factors. It was shown that the shear strengths of specimens were estimated combining the shear strength of structural walls without openings and Ono's reduction factor. The employed computing method well simulated the test results. It was proved that the method may be applied to structural walls with the opening ratio less than 0.46. Then a two-dimensional FEM analytical model was constructed to simulate the behavior observed in the experiment. The model well simulated lateral load – drift angle relations and damage distribution of wall panels.

KEYWORDS: Multi-story structural wall, eccentric openings, stiffness, shear capacity

1. INTRODUCTION

Multi-story structural walls are frequently adopted as a main seismic resisting element in reinforced concrete buildings. In many cases, they have openings for architectural reasons. However, it is difficult to evaluate the shear capacity and stiffness of structural walls with openings. Evaluation is even more difficult if the openings are eccentrically located. It is a common practice to model structural walls with eccentric openings with a strut and tie model. However, the modeling procedure is not straightforward and necessitates some skills. The Japanese building design standard[1] and guidelines [2] employ reduction factors, which are the function of opening size only. The reduction factor is multiplied to the shear strength and shear stiffness of structural walls without openings to obtain those values with openings. Although the reduction factors are very easy to use, they do not reflect the location and number of openings. It is necessary to build more experimental data to clarify the shear resisting mechanisms.

It is important in this paper to understand the index, η, which expresses the size of the opening and is called the opening ratio. The opening ratio, η, is expressed as:

$$\eta = \max\left\{\sqrt{\frac{h_0 \cdot l_0}{h \cdot l}}, \frac{l_0}{l}\right\} \qquad (1)$$

where h and l is the story height and length, h_0 and l_0 is the opening height and length as shown in Figure 1. Opening ratio, , does not reflect the location of opening.

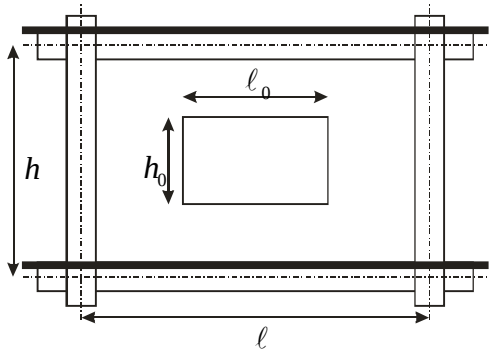

Figure 1 Graphical representation of an opening in a structural wall

2. EXPERIMENT

2.1. Specimens

Four specimens were a 40% scale model of a lower three-story structural wall system taken from the transverse direction of a typical six-story residential building in Japan. The third story was provided for releasing the confinement caused by the stiff loading beam at the top as shown in Figure 2. Test variables were the size and location of openings. N1 had no openings (η=0.0), S1 had small openings (η=0.3), and L1 and L2 had large openings (η=0.46). L2 had a small boundary column at the right side of the openings and this column confines the structural wall panel to increase shear strength and deformation capability. Table 1 shows the section size and reinforcement arrangement common to four specimens. Experimental variables were listed in Table 2. The shear strength reduction factor due to openings was the experimental variable and expressed as follows.

$$\gamma = 1 - \eta \tag{2}$$

AIJ standard [1] requires that the ultimate shear strength of structural wall with opening shall be computed by multiplying γ to the shear strength of structural wall without openings. This reduction concept can be applied as long as the opening ratio is less than 0.4 in AIJ standard. This means that the ultimate shear capacity of N1 and S1 can be obtained in this manner but that of L1 and L2 are required to be computed as a frame composed of columns with a standing wall. Material properties of reinforcement and concrete are listed in Table 3.

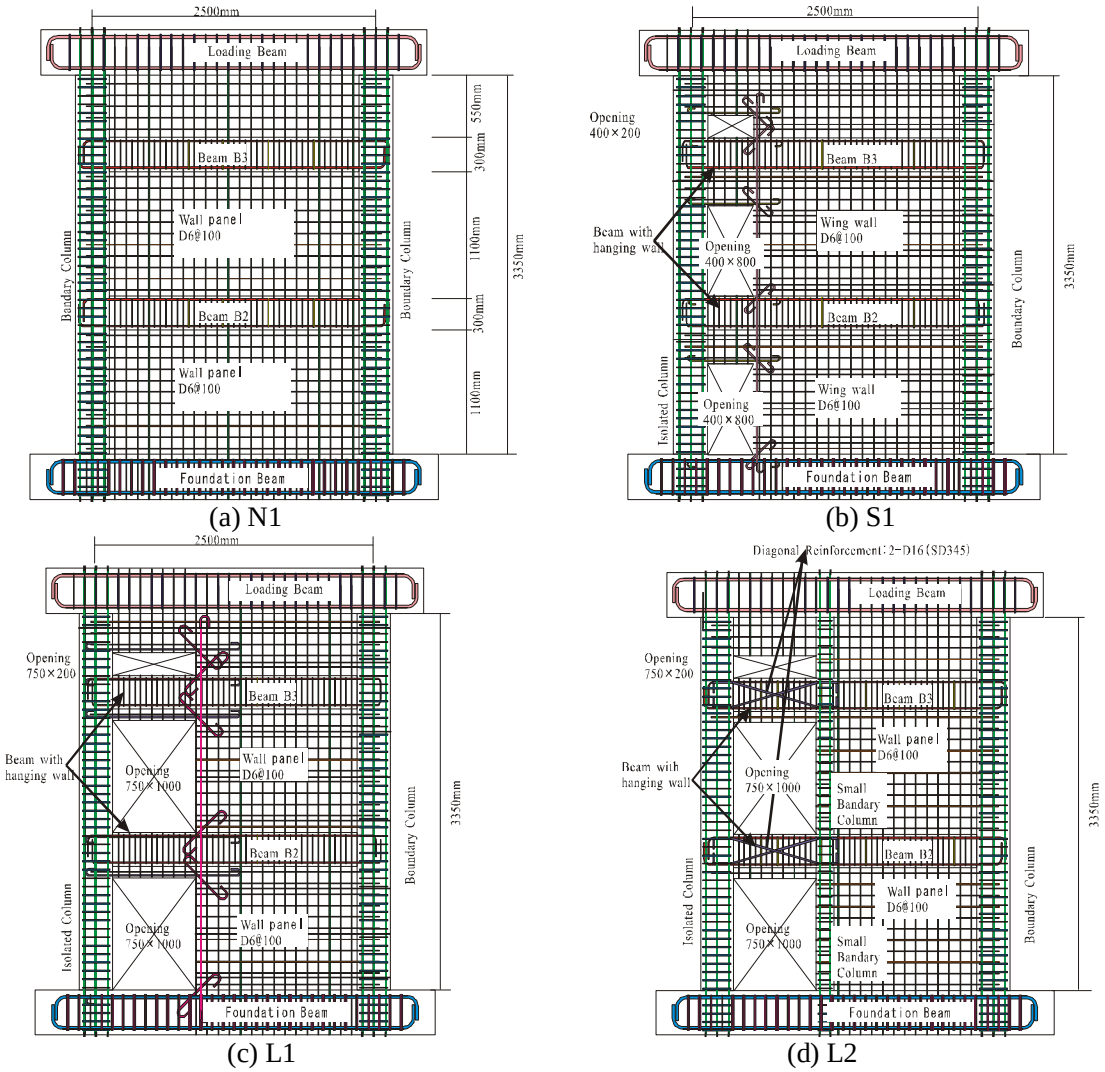

Figure 2 Specimen configurations and reinforcing bar arrangement

Table 1 Section size and reinforcing bars in common

Member	Section size	Longitudinal bar		Shear reinforcement	
		Type	Steel ratio	Type	Steel ratio
Boundary column Isolated column	300×300mm	8-D19	2.55%	2-φ10@75	0.63%
Beam	200×300mm	2-D13	0.47%	2-φ6@100	0.32%
Small Boundary column(L2)	160×160mm	4-D19	4.48%	2-D6@75	0.53%
Wall	t=80mm	D6@100(Staggered) 0.4% in both vertical and horizontal shear reinforcement			

Table 2 Reinforcement arrangement around the openings

Specimen designation	Opening ratio η	Reinforcement around the opening		
		Vertical	Horizontal	Diagonal
N1	0	-	-	-
S1	0.30	1-D13	2-D10	1-D13
L1	0.46	1-D16	2-D13	1-D16
L2	0.46	-	-	-

Table 3 Mechanical Properties

(a) Reinforcing bars

Type	Yield strength (MPa)	Maximum strength (MPa)	Young's modulus (GPa)
D6	425	538	204
D10	366	509	180
D13	369	522	189
D16	400	569	194
D19	384	616	183
φ10	985	1143	197
Separator	1260	1461	759

(b) Concrete

Specimen	Compressive strength (MPa)	Tensile strength (MPa)	Young's modulus (GPa)
N1	25.9	2.3	21.0
S1	25.1	2.2	21.7
L1	28.9	-	26.0
L2	22.0	2.0	22.5

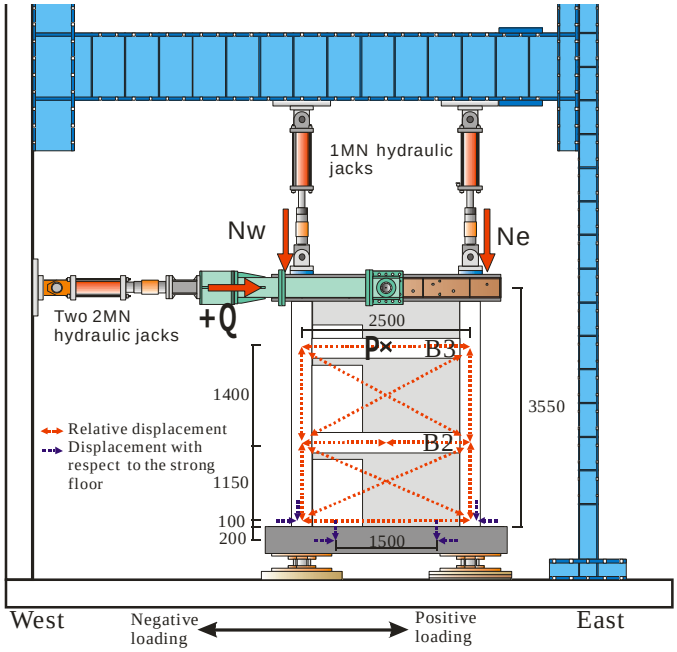

(a) Graphical representation

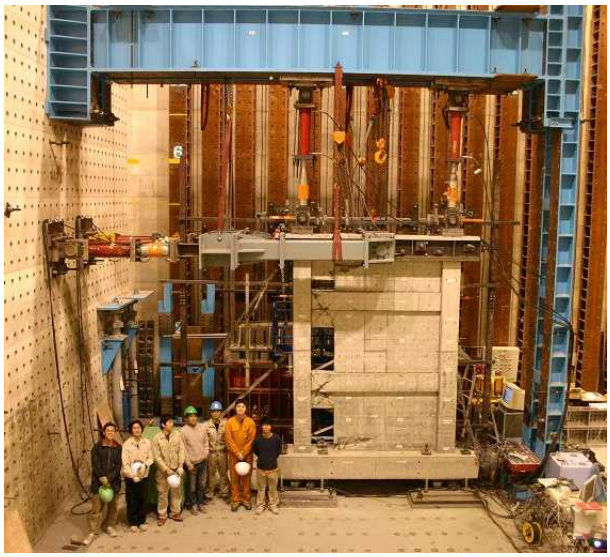

(b) Photographic view

Figure 3 Loading System

2.2. Loading System

Figure 3 shows the loading system. The cyclic reversal lateral load, Q, was applied statically at the midspan of the loading beam through two 2MN hydraulic jacks. Loading was controlled by displacement at P in Figure 3(a) located at the mid-height of beam B3. The loading protocol was two cycles each at drift angles of ±0.05%, ±0.1%, ±0.25%, ±0.5%, ±0.75% and ±1.0%. During the cyclic loading, two vertical 1MN hydraulic jacks were adjusted to keep the contraflexure point at 2500mm above the foundation beam.

$$N_e = 0.42Q + 400kN \quad and \quad N_w = -0.42Q + 400kN \qquad \text{for N1 and S1} \qquad (3)$$

$$N_e = 0.42Q + 244kN \quad and \quad N_w = -0.42Q + 244kN \qquad \text{for L1 and L2} \qquad (4)$$

2.3. Experimental Results

Figure 4 shows the damage observed in the specimen. The shear cracks in the wall and the flexural cracks in the tensile column were observed at R=0.05%, and the number of cracks increased until R=0.5%. The load reached the peak between R=0.5% and 0.75% and damage progressed further after the peak load. At this stage, some longitudinal bars of the beams and the reinforcement of the wall were exposed due to the spalling of cover concrete. The buckling of the wall reinforcement in the first story was also observed. At the final loading stage, the shear sliding of the wall occurred and the strength dropped suddenly. The description above was common for four specimns.

In S1, the shear reinforcement of B2 right above the opening yielded at R=+0.16% and that of B3 yielded at R=-0.46%, and then these beams failed in shear. At R=-0.5%, the concrete at the bottom left corner of the first story crushed, and shear sliding along the foundation took place at R=-1 %. In L1, the shear cracks did not form as much as S1 in the span next to openings. At R=0.5%, the vertical wall reinforcing bars along the opening buckled at the wall base. At R=-1.0%, the shear sliding occurred at the first story but the strength degradation was not as severe as S1. In L2, damage next to the opening was well controlled until the small boundary column at the second story failed in shear below B3 in positive loading, and the failure propagated to the wall panel of the second floor. Higher load was carried before this shear failure but the load level quickly approached to that of L1 after the failure of the small boundary column.

Figure 5 shows the lateral load - drift angle relations until R=1%. Drift angle, R, is defined as the ratio of relative lateral displacement between the top surface of the foundation beam and Point P in Figure 3(a) to its height (2650mm). The peak loads were reached between drift angles of 0.42% and 0.76% in both loading directions as summarized in Table 4. Four specimens showed pinched loops after formation of shear cracks at the wall panels. The intensity of pinching increased as the drift angle increased. It is interesting that the peak load of L2 was reached at larger drift angle compared to the other specimens since the small boundary column next to the openings effectively confined the wall panel and enhanced the deformation capability of the overall structure. Although the peak load was larger in the order of N1, S1, L1, the degradation of load carrying capacity after the peak was also larger in the same order.

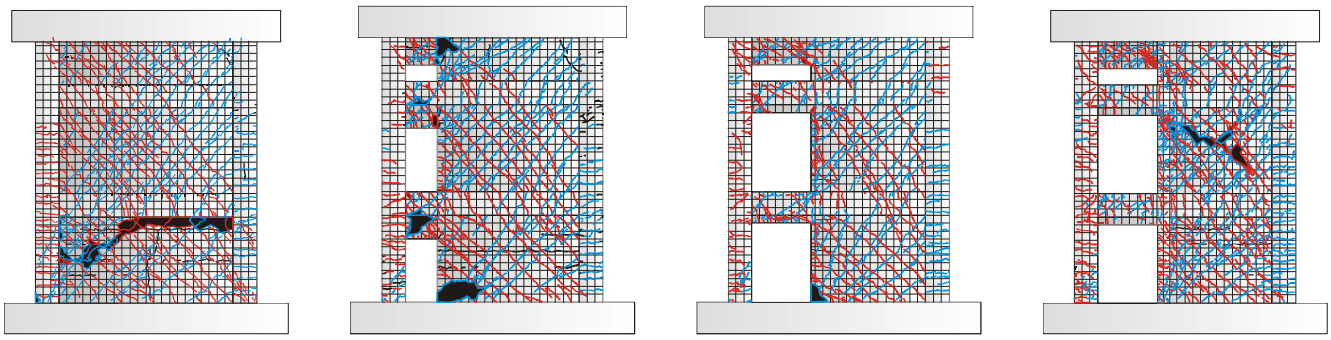

(a) N1 (R=0.75%) (b) S1 (R=0.75%) (c) L1 (R=0.75%) (d) L2 (R=1.0%)

Figure 4 Observed damage of the south face

Table 4 Summary of loading tests and computed results

(a) Positive Direction

Specimen	Experiment			Analysis			Qe/Qc
	Maximum Strength Qe (kN)	Drift Angle (%)	Initial Stiffness (10^5kN/rad)	Maximum Strength Qc (kN)	Drift Angle (%)	Initial Stiffness (10^5kN/rad)	
N1	1179	0.47	16	1140	0.49	8.0	1.03
S1	967	0.46	9.8	929	0.39	6.3	1.04
L1	686	0.68	5.9	752	0.52	5.0	0.91
L2	963	0.76	6.0	766	0.49	5.3	1.26
					Average		1.04
					Standard Deviation		0.11

(b) Negative Direction

Specimen	Experiment			Analysis			Qe/Qc
	Maximum Strength Qe (kN)	Drift Angle (%)	Initial Stiffness (105kN/rad)	Maximum Strength Qc (kN)	Drift Angle (%)	Initial Stiffness (105kN/rad)	
N1	-1039	-0.42	13.4	-1140	-0.49	8.0	0.91
S1	-838	-0.44	11.7	-857	-0.41	6.2	0.98
L1	-649	-0.74	6.7	-690	-0.53	5.0	0.94
L2	-810	-0.75	5.3	-686	-0.5	5.3	1.18
						Average	0.98
						Standard Deviation	0.09

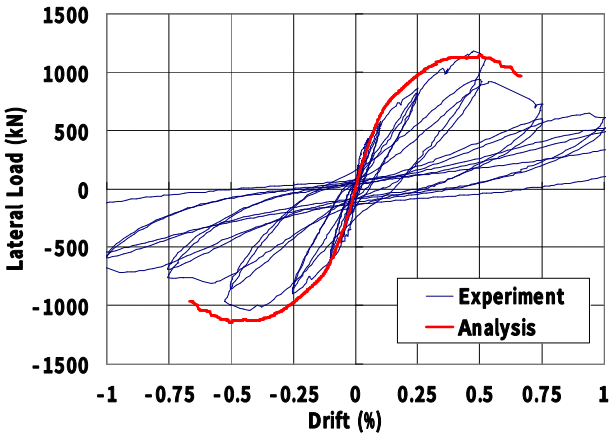

(a) N1

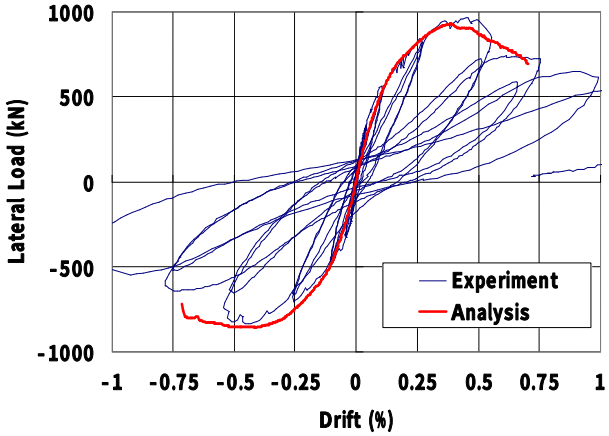

(b) S1

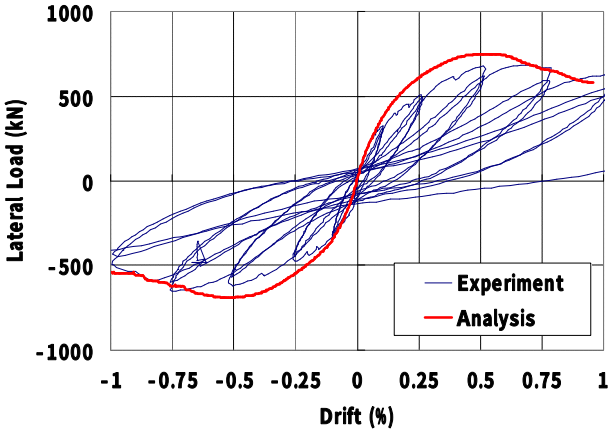

(c) L1

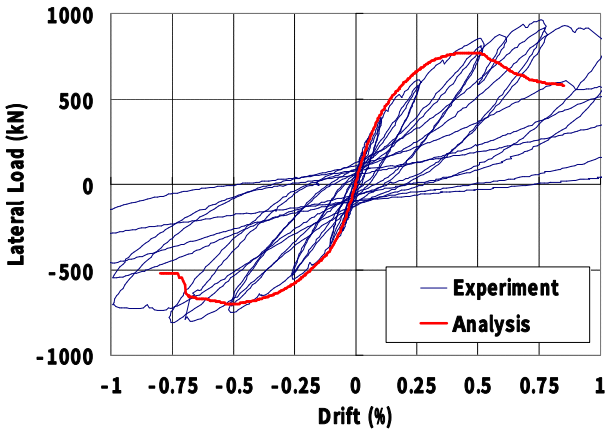

(d) L2

Figure 5 Lateral load – drift angle relationship

3. PREDICTION OF SHEAR CAPACITIES

In Japan, a simple estimation is used to estimate the shear strength of structural walls with openings, Q_s, as follows.

$$Q_s = r_u \cdot V_u \tag{5}$$

where r_u is the reduction factor due to openings and V_u is the shear strength of a structural wall without openings [1]. In this paper, the reduction factor, r_u, proposed by Ono et al. [3] was used based on the compression field of the concrete panel as shown in Figure 6.

$$r_u = 1 - \sqrt{\left(\sum A_e\right)/hl} \tag{6}$$

where, A_e is the area of a diagonal compression field as shown in Figure 6, and h is the distance between the upper and lower beams and l is the distance between two boundary columns. Ono's reduction factor takes into account the location of openings as well as their size. Computed shear strengths, Q_s, are compared with experimental results, Q_{exp}, in Figure 7. Both axes are normalized by the flexural strength, Q_f, computed based on the ACI stress block. It can be seen that the simple estimation using Eq. (5) agrees well with the test results.

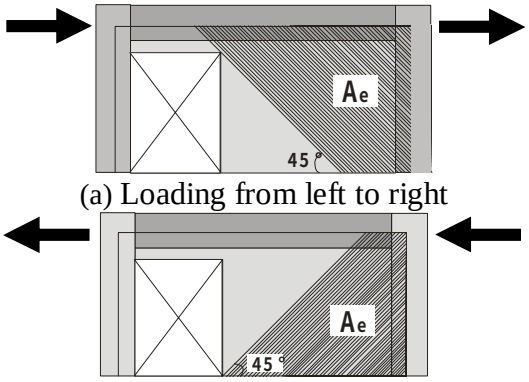

(a) Loading from left to right

(b) Loading from right to left

Figure 6 Assumed area of diagonal compression field

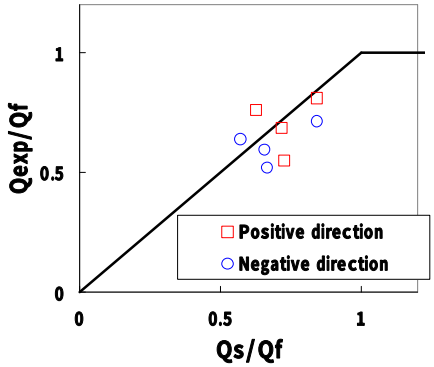

Figure 7 Comparison between the analytical and experimental shear strengths

4. FEM ANALYSIS

4.1. Analytical model

In order to simulate the restoring force characteristics and damage, a pushover analysis was carried out using a two-dimensional FEM analysis program. Figure 8 shows the finite element mesh which employed eight-node quadrilateral isoperimetric elements with nine gauss points. The element size was 200×200mm in wall panels, 200×60mm in beams, 200×100mm in columns. Horizontal and vertical reinforcement was smeared assuming a perfect bond but diagonal reinforcement was neglected. The loading beam and the foundation beam were assumed to be elastic. The concrete constitutive law adopted for cracked concrete is based on the tension stiffening model [4], the compression model [5] and the shear transfer model [6]. Stress-stain relationship of reinforcement was assumed to be bi-linear as shown in Figure 10. Local discontinuities, such as pulling out of reinforcing bars from thicker elements, shear slipping of thinner elements with respect to thicker elements, take place as a result of abrupt changes in the section stiffness at the interface connecting two elements of different thicknesses. Hence, reinforced concrete joint elements were introduced at a boundary between wall panels and columns as well as between wall panels and beams.

4.2. Analytical Results

Analytical lateral load - drift angle relations are compared with test results in Figure 5. The analytical results agreed well with the envelops of experimental results except L2. The simulated peak loads and the corresponding drift angles are compared with the test results in Table 4. Computed initial stiffnesses were smaller than the experimental results. However, the trend of reduction of stiffness with the increase of opening size was well captured. The simulated shear strength of L2 was smaller than the experimental value because the confining effect of small boundary column on the wall panel was not accurately modeled. The analytical simulation of L2 is basically identical to that of L1.

Figure 11 shows simulated damage distribution at the peak load for L1 and L2. The most damaged element was enclosed in a circle. Shear strain concentrated at the first story of wall in L1 but shear strain concentrated at the second story in L2. In experiment, the shear sliding of wall panel occurred at the first story in L1 and at the second story in L2. It is considered that the analytical model well simulated damage as well.

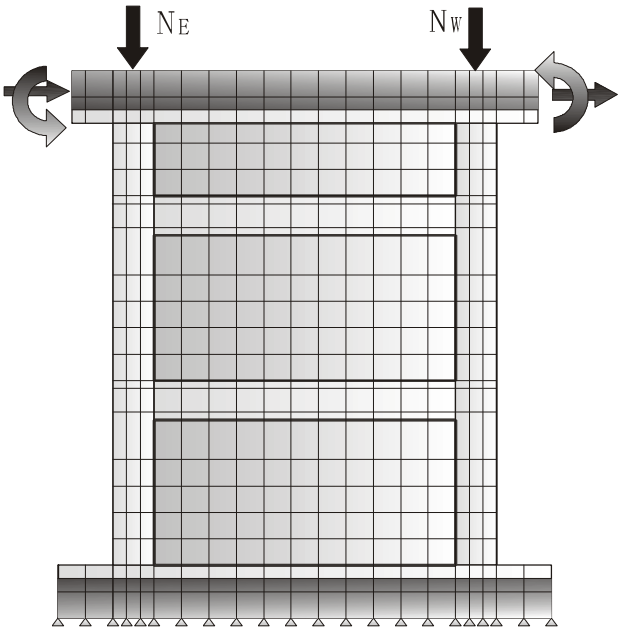

Figure 8 Finite element mesh for N1

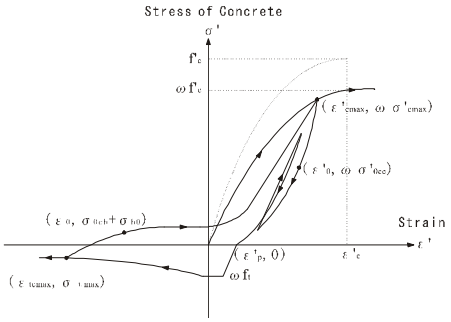

Figure 9 Concrete Constitutive Low [5]

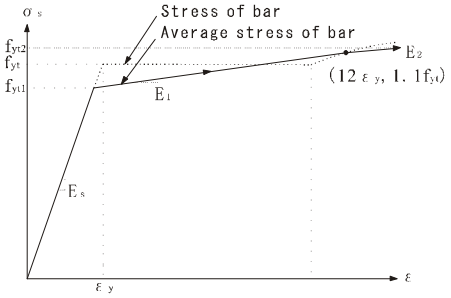

Figure 10 Reinforcement Stress-Strain Relation for steel reinforcement

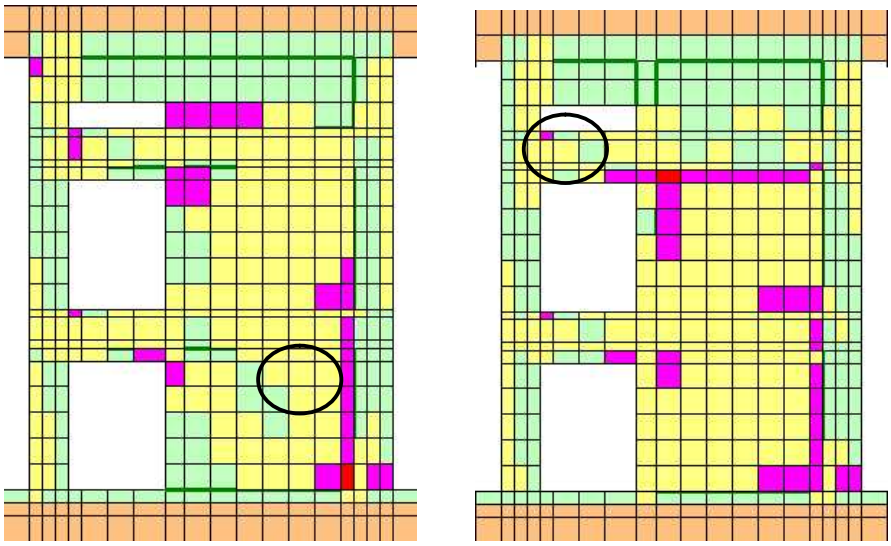

(a) L1 (b) L2

Figure 11 Damage distribution at the peak load

5. CONCLUSIONS

Static loading test was conducted on four 40%-scale specimens in order to evaluate the shear transfer mechanisms of structural walls with eccentric openings.

- Analytical shear strengths were computed combining the shear strength of structural walls without openings and Ono's reduction factor. The employed computing method well simulated the experimental shear strengths. This method may be applied to structural walls with the opening ratio less than 0.46.
- In order to simulate the behavior observed in the experiment, a two-dimensional FEM model was constructed. The analytical model well simulated lateral load – drift angle relations and damage distribution of wall panels.

ACKNOWLEDGEMENT

A part of this research was financially supported by Miracle Three Corporation and Grant-in-aid, Ministry of Education, Culture, Sports, Science and Technology (PI: H. Tanaka). The authors appreciate J. Wang, K. Mori and M. Doi for their great assistance in the experimental works and data processing.

REFERENCES

[1] Architectural Institute of Japan, 1999, "AIJ Standard for Structural Calculation of Reinforced Concrete Structures Based on Allowable Stress Concept"
[2] Architectural Institute of Japan, 2004, "Guidelines for Performance Evaluation of Earthquake Resistant Reinforced Concrete Buildings"
[3] Ono. M, 1995, "Experimental Study on Reinforced Concrete Opening Wall above Opening Periphery Ratio 0.4" Part 1~Part2, Summaries of Technical Papers of Annual Meeting Architectural Institute of Japan C-2, Structures IV 147-150
[4] Shima, H., Okamura, H. and CHOU, L. L., Bond - slip - strain relationship of deformed bars embedded in massive concrete, Journal of Materials, Concrete Structures and Pavements, JSCE, Vol. 378, No. 6, pp. 165 – 174.
[5] Okamura, H. and Maekawa, H, 1991, Nonlinear Analysis and Constitutive Models of Reinforced Concrete, Gihodo Shuppan Co., Ltd.
[6] Li, B. and Maekawa, K., 1988, Stress Transfer Constitutive Equation for Cracked Plane of Concrete Based on the Contact Plane Density Function, Concrete Journal, JCI, Vol. 26, No. 1, pp. 123 – 137, January.
[7] Nishio, H. and Ono, M., 1997, "Study on Shearing Rigidities of Reinforced Concrete framed Shear Walls with Openings" Summaries of Technical Papers of Annual Meeting Architectural Institute of Japan C-2, Structures IV 167-168
[8] The Japan Building Disaster Prevention Association, 2001, "Seismic Evaluation Standards, Guidelines for Existing Reinforced Concrete Buildings"